Appl. Math. Mech. -Engl. Ed., **43**(10), 1615–1630 (2022)

APPLIED MATHEMATICS AND MECHANICS (ENGLISH EDITION)

https://doi.org/10.1007/s10483-022-2902-6

Dynamics of Rossby solitary waves with time-dependent mean flow via Euler eigenvalue model*

Zhihui ZHANG[1], Liguo CHEN[2], Ruigang ZHANG[1,†], Liangui YANG[1], Quansheng LIU[1]

1. School of Mathematical Sciences, Inner Mongolia University, Hohhot 010021, China;
2. School of Statistics and Mathematics, Inner Mongolia University of Finance and Economics, Hohhot 010070, China

(Received Apr. 15, 2022 / Revised Jun. 28, 2022)

Abstract The investigation on the fluctuations of nonlinear Rossby waves is of great importance for the understanding of atmospheric or oceanic motions. The present paper mainly deals with the well-known atmospheric blocking phenomena through the nonlinear Rossby wave theories and the corresponding methods. Based on the equivalent barotropic potential vorticity model in the β-plane approximation underlying a weak time-dependent mean flow, the multiscale technique and perturbation approximated methods are adopted to derive a new forced Korteweg-de Vries model equation with varied coefficients (vfKdV) for the Rossby wave amplitude. For a further analytical treatment of the obtained model problem, a special kind of basic flow is adopted. The evolution processes of atmospheric blocking are well discussed according to the given parameters according to the dipole blocking theory. The effects of some physical factors, especially the mean flow, on the propagation of atmospheric blocking are analyzed.

Key words time-dependent mean flow, Euler eigenvalue model, atmospheric blocking, solitary wave

Chinese Library Classification O29
2010 Mathematics Subject Classification 35Qxx

1 Introduction

The earth's environment, on which human activities depend, is mainly the atmosphere covering the whole earth and the oceans, which account for about two-thirds of the earth's surface

* Citation: ZHANG, Z. H., CHEN, L. G., ZHANG, R. G., YANG, L. G., and LIU, Q. S. Dynamics of Rossby solitary waves with time-dependent mean flow via Euler eigenvalue model. *Applied Mathematics and Mechanics* (*English Edition*), **43**(10), 1615–1630 (2022) https://doi.org/10.1007/s10483-022-2902-6

† Corresponding author, E-mail: rgzhang@imu.edu.cn

Project supported by the National Natural Science Foundation of China (Nos. 12102205 and 11762011), the Natural Science Foundation of Inner Mongolia Autonomous Region of China (No. 2020BS01002), the Research Program of Science at Universities of Inner Mongolia Autonomous Region of China (No. NJZY20003), the Scientific Starting Foundation of Inner Mongolia University of China (No. 21100-5185105), and the Innovative Research Team in Universities of Inner Mongolia Autonomous Region of China (No. NMGIRT2008)

©Shanghai University 2022

area. The movements of the atmosphere and oceans have great influence on world developments and human survival. In recent years, the trend of global climate change has become more and more obvious, and many countries and regions have been suffering from extreme weather attacks to some degree in the last decades. Undoubtedly, the frequent occurrence of extreme weather events not only seriously disrupted the global economy, but also exacerbated the crisis of human survival. Since the 1930, breakthroughs have been made in the mechanisms of large-scale atmospheric and oceanic motions[1]. The most famous theoretical work is the atmospheric long wave theory proposed by meteorologist Rossby[2].

Many understandings of atmospheric and oceanic dynamics in mid-latitudes were accepted based on the outstanding quasi-geostrophic (QG) theory proposed by Charney[3]. The QG theory is not only simple in presentation but also successful in explaining large-scale atmospheric and oceanic flows. Many theoretical models for atmospheric blocking phenomena with a canonical time duration of about two weeks were proposed based on the QG theory, e.g., the onset work by Berggren et al.[4]. It has also been pointed out in the literature that the wave processes of atmosphere and oceans are complex nonlinear ones affected by multiple physical factors, among which the spatial shear effects (meridional and zonal) of the mean flow (i.e., background current) play important roles in the movement of large-scale atmosphere and oceans. In addition, the solitary wave theory has been favored by scholars in the research on the dynamics of nonlinear Rossby waves. The existing results show that it is effective to simulate the excitation, development, and decay of atmospheric blocking through the solitary wave models. Long[5] did the pioneering work via the Korteweg-de Vries (KdV) equation to simulate the evolution of Rossby wave amplitude under the β-plane approximation in 1964. Redekopp and Weidman[6] studied the generation of Rossby solitary waves in shear flow, and pointed out the necessary conditions for the existence of Rossby solitary waves in zonal flow. Subsequently, essential improvements were made on the theoretical treatments of the atmospherical blocking. Charney and Devore[7] initiated the multiple flow equilibria to characterize the evolution of atmospheric blocking. McWilliams[8] successfully analyzed the blocking by using the equivalent modons theory. Shutts[9] held the opinion that it was the synoptic-scale eddies forcing the steady state of the atmospheric blocking. Malguzzi and Malanotte-Rizzoli[10] proposed to use the solitary wave solution to explain dipole blocking, and pointed out that this idealized model had a strong similarity to the actual observation. Luo and Ji[11] and Luo[12] put forward the envelope Rossby solitary wave theory of the nonlinear Schrödinger type to explain the formation process and decline mechanism of dipole blocking. Luo[13–14] and Luo et al.[15] studied the geographical distribution, seasonal variation, and interannual variation of dipole blocking through observation and analysis. Lu et al.[16] derived a time-fractional generalized Boussinesq equation to describe the evolution of Rossby solitary waves under dissipation. Zhang and Yang[17], Wang et al.[18–19], and Zhang et al.[20] investigated the dynamics of Rossby waves under zonal shear background flow and the nonlinear barotropic-baroclinic coherent structure interaction by using the coupled nonlinear evolution model equations systematically. Ciro et al.[21] characterized the atmospheric blocking via single-triad of Rossby-Haurwitz waves perturbed by one topographic mode. Shi et al.[22–23] discussed the effect of the background flow on the topographic Rossby waves, and the corresponding theoretical results support a potential explanation for the propagation speeds and distributions of eddies along the Kuroshio current in the East China Sea.

The instability problem is always an attracting topic for the researchers. Solomon et al.[24] studied the instability of the shear flow of rotating fluid. Hodyss and Nolan[25] considered the behavior of vortex Rossby (VR) waves undergoing inertia-buoyancy (IB) wave emission on vortices with baroclinic vertical structures. Kalashnik et al.[26] investigated the linear stability of jet flows induced by piecewise constant boundary distributions of buoyancy based on the two-layer lever surface quasigeostrophic model. Zhang et al.[27] and Yang and Song[28] discussed the effects of shear basic flow and topography in inducing the instability of the Rossby wave.

With the deepening of research, scholars realize that not only the spatial shear effect of basic flow has an important effect on large-scale atmospheric and ocean fluctuations, but also the temporal variation of basic flow has attracted their attention. Berloff and McWilliams[29] analyzed the linear stability and nonlinear time-varying characteristics of the western boundary flow. The results showed that the flow lost stability at medium Reynolds numbers, and the stability threshold strongly depended on the vertical stratification profile. In the cases of no slip and free slip, the finite amplitude dynamics was fundamentally different, because the free slip boundary basically stabilized the flow. The fluctuation of nonlinear region is very different from that of a linear instability model. In this century, Poulin[30] began to study the large-scale atmospheric and oceanic wave mechanism under the action of time-varying oscillatory basic flow. Huang et al.[31] discussed the atmospheric blocking phenomena under the action of time-varying basic flow. Radko[32] studied the long wave instability of inviscid parallel time-varying current on the β plane, and showed that the existence of fluctuation component, no matter how weak it was, always made the basic current linearly unstable. This instability is caused by the resonant forcing of large-scale Rossby waves. The analysis is based on the asymptotic multiscale model and verified by numerical simulation. Since most geophysical flows are time-dependent, the associated shear instability may be an important and widespread source of barotropic turbulence[32–33]. Yan et al.[34] considered the energy problem of eddy current under the action of boundary flow. The results showed that for time-uniform and time-varying flow fields, all energy components and transformations distributed unevenly. There are also relevant studies on this topic[35–36].

In view of the essential roles of the background flow in atmosphere and oceans, the present paper mainly focuses on the study of the atmospheric blocking underlying time-dependent mean-flow. The rest of the paper is organized as follows. In Section 2, a new forced Korteweg-de Vries model equation with variable coefficients (vfKdV) is obtained based on the conserved potential vorticity model. In Section 3, the evolution of nonlinear Rossby solitary waves are analyzed in detail via the classical Sturm-Liouville eigenvalue problem characterized by the well-known Euler model equation. Finally, in Section 4, the conclusions are presented.

2 Models and methods

2.1 Control model equation and boundary conditions

The nondimensional nonlinear equivalent barotropic vorticity equation under the β-plane approximation is adopted as[31]

$$\Big(\frac{\partial}{\partial t}+u\frac{\partial}{\partial x}+v\frac{\partial}{\partial y}\Big)\Big(\frac{\partial v}{\partial x}-\frac{\partial u}{\partial y}-F\psi\Big)+\beta\frac{\partial \psi}{\partial x}=0. \tag{1}$$

$F=L^2/R_0^2$ is the Froude number, where $L=10^6\,\mathrm{m}$ is the characteristic length scale and R_0 is the Rossby deformation radius. $\beta=\beta_0L^2/U$, where $\beta_0=2\omega_0\cos\phi_0/a_0$ is the Rossby parameter denoting the essential importance on the atmosphere or oceans from the earth's rotation in which $U=1\,\mathrm{m}\cdot\mathrm{s}^{-1}$ means the characteristic velocity scale, and ω_0 represents the angular frequency of the earth's rotation, a_0 is the earth's radius, and ϕ_0 means the latitude. ψ is the streamfunction. $u=-\frac{\partial\psi}{\partial y}$ and $v=\frac{\partial\psi}{\partial x}$ are given according to the impressibility of the fluids.

The dimensionless non-penetration boundary conditions are

$$\frac{\partial\psi}{\partial x}=0,\quad y=0,y_0. \tag{2}$$

2.2 Derivation of vfKdV

The streamfunction is defined as

$$\psi(x,y,t)=\psi_0(y,t)+\psi'(x,y,t), \tag{3}$$

where $\psi_0 = U_0(y) + \sum\limits_{n=1}^{\infty} \epsilon^n U_n(y,t)$ represents the time-dependent mean flow, and $\psi'(x,y,t) = \sum\limits_{n=1}^{\infty} \epsilon^n \psi'_n(x,y,t)$ is the disturbed one. $u = -\big(\frac{\partial \psi_0}{\partial y} + \frac{\partial \psi'}{\partial y}\big) = \overline{u} + u'$ and $v = \frac{\partial \psi_0}{\partial x} + \frac{\partial \psi'}{\partial x} = v'$ are the velocities correspondingly.

Due to the properties of both multiple scales and high nonlinearity for large-scale atmospheric motions, introduce the following Gardner-Morikawa transform:

$$\xi = \epsilon^{1/2}(x - c_0 t), \quad \tau = \epsilon^{3/2} t. \tag{4}$$

The upper prime notations of the perturbed terms are omitted without any confusion in what follows. Substituting Eq. (4) into Eqs. (1) and (2) yields

$$\begin{cases} \Big(\epsilon^2 \dfrac{\partial}{\partial \tau} - \epsilon c_0 \dfrac{\partial}{\partial \xi}\Big) \dfrac{\partial^2 \psi}{\partial \xi^2} + \Big(\epsilon \dfrac{\partial}{\partial \tau} - c_0 \dfrac{\partial}{\partial \xi}\Big) \dfrac{\partial^2 \psi}{\partial y^2} - \epsilon F \dfrac{\partial \psi}{\partial \tau} + F c_0 \dfrac{\partial \psi}{\partial \xi} - \epsilon \dfrac{\partial \psi}{\partial y} \dfrac{\partial^3 \psi}{\partial \xi^3} \\ - \dfrac{\partial \psi}{\partial y} \dfrac{\partial^3 \psi}{\partial y^2 \partial \xi} + \epsilon \dfrac{\partial \psi}{\partial \xi} \dfrac{\partial^3 \psi}{\partial \xi^2 \partial y} + \dfrac{\partial \psi}{\partial \xi} \dfrac{\partial^3 \psi}{\partial y^3} + \beta \dfrac{\partial \psi}{\partial \xi} = 0, \\ \dfrac{\partial \psi}{\partial \xi} = 0, \quad y = 0, y_0. \end{cases} \tag{5}$$

According to the rule of weak nonlinear perturbation expansions, the zeroth-order equations of ϵ are satisfied with

$$\begin{cases} - c_0 \dfrac{\partial^3 U_0}{\partial \xi \partial y^2} + F c_0 \dfrac{\partial U_0}{\partial \xi} - \dfrac{\partial U_0}{\partial y} \dfrac{\partial^3 U_0}{\partial y^2 \partial \xi} + \dfrac{\partial U_0}{\partial \xi} \dfrac{\partial^3 U_0}{\partial y^3} + \beta \dfrac{\partial U_0}{\partial \xi} = 0, \\ \dfrac{\partial U_0}{\partial \xi} = 0, \quad y = 0, y_0. \end{cases} \tag{6}$$

Obviously, Eq. (6) is an identity.

The first-order equation of ϵ is

$$\begin{cases} - c_0 \dfrac{\partial^3 \psi_1}{\partial \xi \partial y^2} + F c_0 \dfrac{\partial \psi_1}{\partial \xi} - \dfrac{\mathrm{d} U_0}{\mathrm{d} y} \dfrac{\partial^3 \psi_1}{\partial y^2 \partial \xi} + \dfrac{\partial \psi_1}{\partial \xi} \dfrac{\mathrm{d}^3 U_0}{\mathrm{d} y^3} + \beta \dfrac{\partial \psi_1}{\partial \xi} = 0, \\ \dfrac{\partial \psi_1}{\partial \xi} = 0, \quad y = 0, y_0. \end{cases} \tag{7}$$

Equation (7) proposes an assumed ψ_1 with the following separated variable form:

$$\psi_1 = A(\xi, \tau) G(y, \tau). \tag{8}$$

Substitution of Eq. (8) into Eq. (7) yields

$$\begin{cases} \Big(\dfrac{\mathrm{d} U_0}{\mathrm{d} y} + c_0\Big) \dfrac{\partial^2 G}{\partial y^2} - \Big(F c_0 + \dfrac{\mathrm{d}^3 U_0}{\mathrm{d} y^3} + \beta\Big) G = 0, \\ G(0) = G(y_0) = 0. \end{cases} \tag{9}$$

The second-order equation of ϵ is

$$\begin{cases} \quad - c_0 \dfrac{\partial^3 \psi_2}{\partial \xi \partial y^2} + F c_0 \dfrac{\partial \psi_2}{\partial \xi} - \dfrac{\mathrm{d} U_0}{\mathrm{d} y} \dfrac{\partial^3 \psi_2}{\partial y^2 \partial \xi} + \dfrac{\partial \psi_2}{\partial \xi} \dfrac{\mathrm{d}^3 U_0}{\mathrm{d} y^3} + \beta \dfrac{\partial \psi_2}{\partial \xi} \\ = - \Big(- c_0 \dfrac{\partial^3 \psi_1}{\partial \xi^3} + \dfrac{\partial^3 \psi_1}{\partial \tau \partial y^2} + \dfrac{\partial^3 U_1}{\partial \tau \partial y^2} - F \dfrac{\partial \psi_1}{\partial \tau} - F \dfrac{\partial U_1}{\partial \tau} - \dfrac{\mathrm{d} U_0}{\mathrm{d} y} \dfrac{\partial^3 \psi_1}{\partial \xi^3} - \dfrac{\partial U_1}{\partial y} \dfrac{\partial^3 \psi_1}{\partial y^2 \partial \xi} \\ \quad + \dfrac{\partial \psi_1}{\partial \xi} \dfrac{\partial^3 \psi_1}{\partial y^3} + \dfrac{\partial \psi_1}{\partial \xi} \dfrac{\partial^3 U_1}{\partial y^3} - \dfrac{\partial \psi_1}{\partial y} \dfrac{\partial^3 \psi}{\partial y^2 \partial \xi}\Big), \\ \dfrac{\partial \psi_2}{\partial \xi} = 0, \quad y = 0, y_0. \end{cases} \tag{10}$$

Take $\psi_2 = 0$, and substitute $\psi_1 = A(\xi, \tau)G(y, \tau)$ into the first expression of Eq. (10). Then, we have

$$-\Big(c_0 + \frac{\mathrm{d}U_0}{\mathrm{d}y}\Big)G\frac{\partial^3 A}{\partial \xi^3} + \Big(G\frac{\partial^3 G}{\partial y^3} - \frac{\partial G}{\partial y}\frac{\partial^2 G}{\partial y^2}\Big)A\frac{\partial A}{\partial \xi} + \Big(G\frac{\partial^3 U_1}{\partial y^3} - \frac{\partial U_1}{\partial y}\frac{\partial^2 G}{\partial y^2}\Big)\frac{\partial A}{\partial \xi}$$
$$+ \frac{\partial}{\partial \tau}\Big(\Big(\frac{\partial^2 G}{\partial y^2} - FG\Big)A\Big) + \frac{\partial}{\partial \tau}\Big(\frac{\partial^2 U_1}{\partial y^2} - FU_1\Big) = 0. \tag{11}$$

In view of the separated property of variables, it is accepted to multiply both sides of Eq. (11) by y^2. Integrating from 0 to y_0 with respect to y, the vfKdV equation can be written as

$$\frac{\partial A}{\partial \tau} + e_1\frac{\partial^3 A}{\partial \xi^3} + e_2 A\frac{\partial A}{\partial \xi} + e_3\frac{\partial A}{\partial \xi} + e_4 A + e_5 = 0, \tag{12}$$

where

$$\begin{cases} e_1 = \dfrac{\int_0^{y_0} -\big(c_0 + \frac{\mathrm{d}U_0}{\mathrm{d}y}\big)Gy^2\mathrm{d}y}{\int_0^{y_0}\big(\frac{\partial^2 G}{\partial y^2} - FG\big)y^2\mathrm{d}y}, \quad e_2 = \dfrac{\int_0^{y_0}\big(G\frac{\partial^3 G}{\partial y^3} - \frac{\partial G}{\partial y}\frac{\partial^2 G}{\partial y^2}\big)y^2\mathrm{d}y}{\int_0^{y_0}\big(\frac{\partial^2 G}{\partial y^2} - FG\big)y^2\mathrm{d}y}, \\ e_3 = \dfrac{\int_0^{y_0}\big(G\frac{\partial^3 U_1}{\partial y^3} - \frac{\partial U_1}{\partial y}\frac{\partial^2 G}{\partial y^2}\big)y^2\mathrm{d}y}{\int_0^{y_0}\big(\frac{\partial^2 G}{\partial y^2} - FG\big)y^2\mathrm{d}y}, \quad e_4 = \dfrac{\frac{\partial}{\partial \tau}\big(\int_0^{y_0}\big(\frac{\partial^2 G}{\partial y^2} - FG\big)y^2\mathrm{d}y\big)}{\int_0^{y_0}\big(\frac{\partial^2 G}{\partial y^2} - FG\big)y^2\mathrm{d}y}, \\ e_5 = \dfrac{\int_0^{y_0}\frac{\partial}{\partial \tau}\big(\frac{\partial^2 U_1}{\partial y^2} - FU_1\big)y^2\mathrm{d}y}{\int_0^{y_0}\big(\frac{\partial^2 G}{\partial y^2} - FG\big)y^2\mathrm{d}y}. \end{cases} \tag{13}$$

In Eq. (13), $e_i = e_i(\tau)$ $(i = 1, 2, 3, 4, 5)$.

2.3 Analytical solution for vfKdV

From the above derivations, it can be seen that the background flow ψ_0 can be arbitrary. However, in order to obtain the meaningful solution and further to analyze the model, a special background flow is assumed to be

$$U_0(y) = \frac{4}{3}a_1 y^3 - c_0 y, \quad U_1(y, t) = a_2(t)y^2 + a_3(t)y + a_4(t), \quad U_n = 0\ (n \geqslant 2),$$

where a_1 is a constant, and a_2, a_3, and a_4 are functions dependent on time t, i.e., the background flow is

$$\psi_0 = \frac{4}{3}a_1 y^3 - c_0 y + \epsilon(a_2(t)y^2 + a_3(t)y + a_4(t)). \tag{14}$$

Substituting special background flow into the first expression of Eq. (9) yields

$$4a_1 y^2\frac{\partial^2 G}{\partial y^2} - (Fc_0 + 8a_1 + \beta)G = 0. \tag{15}$$

Obviously, this is a classical Euler eigenvalue equation with the solution

$$G = y^{\frac{1}{2}}F_1\sin(M\ln(y) + F_2), \tag{16}$$

where F_1 and F_2 are constants to be determined by boundary conditions, and $c_0 = -(2a_1M^2 + 9a_1+\beta)/F$. Thus, the whole coefficients $e_i = e_i(\tau)$ $(i = 1, 2, 3, 4, 5)$ in Eq. (12) will be calculated. The final step is to find the solutions to Eq. (12). Many scholars have given specific calculation methods, e.g., the homogeneous balance method[37], the Clarkson-Kruskal direct method[38], the F-expansion method[39–40], and the Jacobi elliptic function expansion method[41–42]. Here, the Jacobi elliptic function expansion method is used. First, a traveling wave formal solution is assumed to be

$$A = A(\zeta), \quad \zeta = f(\tau)\xi + g(\tau), \tag{17}$$

where $f(\tau)$ and $g(\tau)$ are undetermined functions varying with time τ. Expand $A(\zeta)$ as the following series for the Jacobi elliptic sine function:

$$A(\zeta) = \sum_{j=0}^{n} a_j(\tau)\mathrm{sn}^j\zeta. \tag{18}$$

Substitute Eqs. (17) and (18) into Eq. (12). Then, in view of the balance between nonlinearity and the highest derivatives, we have the fact $n = 2$. Thus, the solution to Eq. (12) is

$$A(\zeta) = a_0(\tau) + a_1(\tau)\mathrm{sn}\zeta + a_2(\tau)\mathrm{sn}^2\zeta. \tag{19}$$

Bringing Eq. (19) back to Eq. (12) and using the transformation between the three basic Jacobi elliptic functions sn, cn, and dn yield

$$\begin{aligned} & e_5 + a_0' + a_0e_4 + (a_1' + a_1e_4)\mathrm{sn}\zeta + (a_2' + a_2e_4)\mathrm{sn}^2\zeta \\ & + a_1((f'\xi + g') - (1+m^2)e_1f^3 + a_0e_2f + e_3f)\mathrm{cn}\zeta\mathrm{dn}\zeta \\ & + (2a_2(f'\xi + g') - 8(1+m^2)a_2e_1f^3 + (a_1^2 + 2a_0a_2)e_2f + 2a_2e_3f)\mathrm{sn}\zeta\mathrm{cn}\zeta\mathrm{dn}\zeta \\ & + a_1f(6m^2e_1f^2 + 3a_2e_2)\mathrm{sn}^2\zeta\mathrm{cn}\zeta\mathrm{dn}\zeta + 2a_2f(12m^2e_1f^2 + a_2e_2)\mathrm{sn}^3\zeta\mathrm{cn}\zeta\mathrm{dn}\zeta \\ = & \, 0, \end{aligned} \tag{20}$$

where $0 < m < 1$ is the module, and

$$\begin{cases} e_5 = 0, \\ a_0' + a_0e_4 = 0, \quad a_1' + a_1e_4 = 0, \quad a_2' + a_2e_4 = 0, \\ a_1((f'\xi + g') - (1+m^2)e_1f^3 + a_0e_2f + e_3f) = 0, \\ 2a_2(f'\xi + g') - 8(1+m^2)a_2e_1f^3 + (a_1^2 + 2a_0a_2)e_2f + 2a_2e_3f = 0, \\ a_1f(6m^2e_1f^2 + 3a_2e_2) = 0, \\ 2a_2f(12m^2e_1f^2 + a_2e_2) = 0. \end{cases} \tag{21}$$

Equation (21) can be solved with

$$\begin{cases} a_0 = C_1\mathrm{e}^{-\int_0^\tau e_4\mathrm{d}t}, \quad a_1 = 0, \quad a_2 = -\dfrac{12m^2e_1f^2}{e_2}, \\ f = k, \quad g = \displaystyle\int_0^\tau 4(1+m^2)e_1f^3 - \Big(\frac{a_1^2}{2a_2} + a_0\Big)e_2f - e_3f\mathrm{d}t, \end{cases} \tag{22}$$

where k and C_1 are arbitrary constants. Then, Eq. (19) becomes

$$A = C_1\mathrm{e}^{-\int_0^\tau e_4\mathrm{d}t} - \frac{12m^2e_1k^2}{e_2} + \frac{12m^2e_1k^2}{e_2}\mathrm{cn}^2\zeta, \tag{23}$$

where $\zeta = k\xi + \int_0^\tau \big(4(1+m^2)e_1k^3 - C_1\mathrm{e}^{-\int_0^\tau e_4\mathrm{d}t}e_2k - e_3k\big)\mathrm{d}t$. When $m \to 1$, $\mathrm{cn}\zeta \to \mathrm{sech}\zeta$, and the final solution will be

$$A = C_1\mathrm{e}^{-\int_0^\tau e_4\mathrm{d}t} - \frac{12e_1k^2}{e_2} + \frac{12e_1k^2}{e_2}\mathrm{sech}^2\Big(k\xi + \int_0^\tau (8e_1k^3 - C_1\mathrm{e}^{-\int_0^\tau e_4\mathrm{d}t}e_2k - e_3k)\mathrm{d}t\Big). \tag{24}$$

3 Results

From the solution process of Eq. (12), we know that $e_5 = 0$, from which we can deduce $a_4 = \frac{2}{F}a_2 - \frac{3}{5}a_2y_0^2 - \frac{3}{4}a_3y_0$. The approximated solution to Eq. (1) can be obtained by substituting

Eqs. (4) and (8) and the special background flow into Eq. (3) as follows:

$$\psi = \frac{4}{3}a_1y^3 + \epsilon a_2y^2 + (\epsilon a_3 - c_0)y + \left(\frac{2}{F} - \frac{3}{5}y_0^2\right)\epsilon a_2 - \frac{3}{4}y_0\epsilon a_3 + \left(C_1 - \frac{3(C_1e_2+e_3)}{2e_2} + \frac{3C_1e_2+e_3}{2e_2}\mathrm{sech}^2(k\epsilon^{1/2}(x-c_0t))\right)\epsilon y^{1/2}F_1\sin(M\ln(y)+F_2). \tag{25}$$

Predecessors have given a specific definition of dipole blocking, and pointed out that dipole blocking in the atmosphere mainly occurs in the range from 60°N to 70°N, and most of the dipole blocking occurs near 60°N[11–12]. Therefore, we take ϕ_0 to be 60°N. According to the previous derivation, $c_0 = -(2a_1M^2 + 9a_1 + \beta)/F$ can be known, and $c_0 > 0$ can be obtained when $a_1 < -\frac{\beta}{2M^2+9}$ is satisfied. Figure 1 can be obtained by taking other parameters as $y_0 = 3$, $F_1 = 2.5$, $F_2 = 2\pi t$, $\epsilon = 0.1$, $a_1 = -0.5$, $a_2 = -0.2\cos(1.2t)$, $a_3 = -2\cos(1.2t)$, $C_1 = -54$, $F = 64^2$, $M = \frac{\pi}{\ln y_0}$, and $k = 2$. It shows the evolution of two pairs of dipole blocking over time. At $t = 0$, the background westerly flow splits into three branches, producing two pairs of dipoles. However, near $y = 0$, there is no gentle westerly flow in the figure, which may be due to the singularity of the approximate solution to the streamfunction, Eq. (25), at $y = 0$. It is obvious that dipole blocking increases firstly and then decreases with time. In addition, the evolution of more dipole blocking can be seen in the figure when M is larger. The property of dipole blocking is general, and we will discuss only one pair of dipoles.

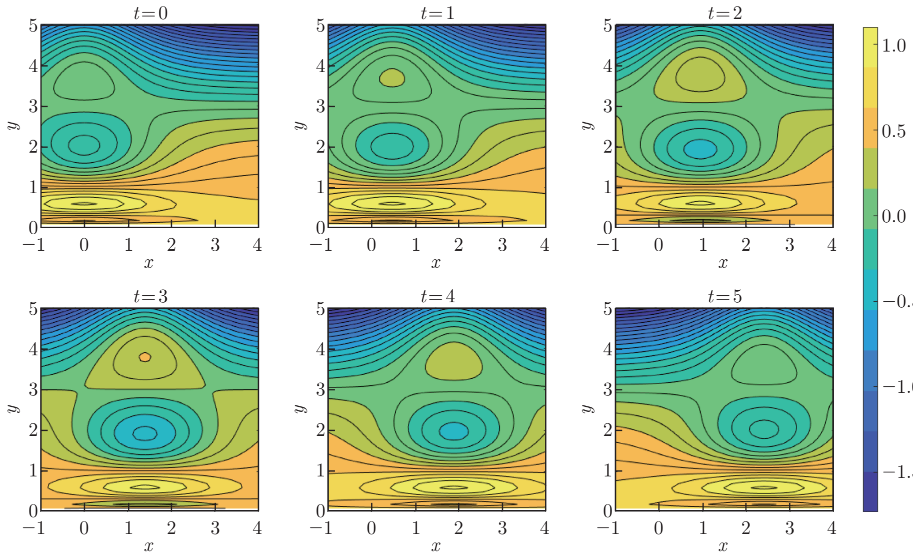

Fig. 1 Evolution of dipole blocking under the given parameters (color online)

3.1 Effect of uniform zonal mean flow

The zonal background flow can be obtained from Eq. (14) because

$$\overline{u} = -\frac{\partial\psi_0}{\partial y} = \overline{u}_0 + Q(y), \tag{26}$$

where $\overline{u}_0 = c_0 - \epsilon a_3(t)$ stands for the mean zonal background flow. $Q(y) = -4a_1y^2 - 2\epsilon a_2(t)y$ is a quadratic function, which indicates that the background flow shear is nonlinear. From the previous analysis, c_0 is a function depending on a_1. Therefore, combining with Eq. (26), it can be seen that when a_1 changes, the mean zonal background flow $\overline{u}_0$ and shear $Q(y)$ will change simultaneously. Let the other parameters remain unchanged, and consider the constraints of

a_1 mentioned earlier. Then, when a_1 changes from -0.5 to -0.7 (set as $a_1 = -0.5$, $a_1 = -0.6$, and $a_1 = -0.7$, respectively), it represents the strengthening of the background westerly flow. The evolution of dipole blocking is shown in Fig. 2. When $a_1 = -0.4, -0.3$, or -0.2, A changes from -0.4 to -0.2. When $a_3 = 2\cos(1.2t)$, the background easterly flow is strengthened. The dipole blocking is shown in Fig. 3.

It can be seen from Fig. 2 that when the background westerly flow is strengthened, the movement velocity of dipole blocking is significantly accelerated. However, Fig. 3 shows that when the background easterly flow intensifies, the movement speed of the dipole blocking slows down. Considering the evolution of dipole blocking on a given day, it is not difficult to find that the intensity of dipole blocking decreases with the strengthening of the background westerly flow. This shows that under the condition of nonlinear shear, dipole blocking is more likely to occur in weak background westerly flow. Luo[43] showed that dipole blocking mainly existed in weak westerly flow when the role of background westerly flow shear and other factors were not taken into account. Luo and Xu[44] studied theoretically, and concluded that appropriate weak westerly flow was crucial to the formation of blocking and strong background westerly flow was not conducive to the formation of blocking. The background westerly conditions considered in this paper are different from those of our predecessors, but the conclusions obtained are the same and also agree with the actual observation results. This provides another strong basis for the result that the weak background westerly flow is more favorable to the formation of dipole blocking. In addition, Fig. 3 shows that when the background easterly flow intensifies, the dipole blocking also intensifies. This indicates that strong easterly flow is more favorable to the formation of dipole blocking, which is contrary to the conclusion obtained under the condition of westerly flow. From the previous analysis, it can be seen that in the absence of background flow, the dipole blocking moves westward.

3.2 Effect of shear mean flow

As discussed earlier, the nonlinear shear $Q(y)$ depends on a_1 and $a_2(t)$. The change of a_1 will cause the change of the mean zonal background flow. Therefore, the value of a_1 is fixed as a constant, and the effect of shear on dipole blocking is discussed by changing the value of a_2. Consider the simple model first, let a_2 be a constant, and take the shear as $a_2 = -0.01$, -0.3, -0.6, and -1.0, respectively. The effects of westerly ($a_1 = -0.5$ and $a_3 = -2\cos(1.2t)$) shear and easterly ($a_1 = -0.4$ and $a_3 = 2\cos(1.2t)$) shear are considered at $t = 2$, as shown in Figs. 4 and 5, respectively. Next, change a_2 into a function of time, and take the shear as $a_2 = -0.3\cos(1.2t)$, $-0.6\cos(1.2t)$, and $-0.9\cos(1.2t)$, respectively. The effects of westerly ($a_1 = -0.5$ and $a_3 = -2\cos(1.2t)$) shear and easterly ($a_1 = -0.4$ and $a_3 = 2\cos(1.2t)$) shear are also considered on the second day, as shown in Figs. 6 and 7, respectively.

In the first case, the shear of the background flow is constant. Figure 4 shows that when the westerly shear increases, i.e., a_2 changes from -0.01 to -1.0, the intensity of dipole blocking decreases and the center of high pressure and low pressure gradually disappears. As can be seen from Fig. 5, the background easterly shear has the same conclusion as the westerly shear, i.e., the dipole blocking decreases when the shear of the background zonal flow increases. This shows that the weak nonlinear shear is favorable to the formation of dipole blocking. In addition, from Figs. 4 and 5, it can be seen that, when a_2 takes the same value, the intensity of dipole blocking is slightly stronger under the background easterly shear condition, indicating that easterly shear is more conducive to the generation of dipole blocking than westerly shear.

In the second case, the shear of the background flow is a function of time. Figures 6 and 7 further verify the previous conclusion when the shear is constant. Besides, the two figures also indicate that for both the background westerly shear and easterly shear, the increase (a_2 changes from $-0.3\cos(1.2t)$ to $-0.9\cos(1.2t)$) in shear makes the blocking weaker when dipole blocking is weak (see the figures on $t = 0$) while even stronger when dipole blocking is strong (see the figures on $t = 0$). This results in more pronounced dipole blocking generation and decay processes as the time-dependent shear increases.

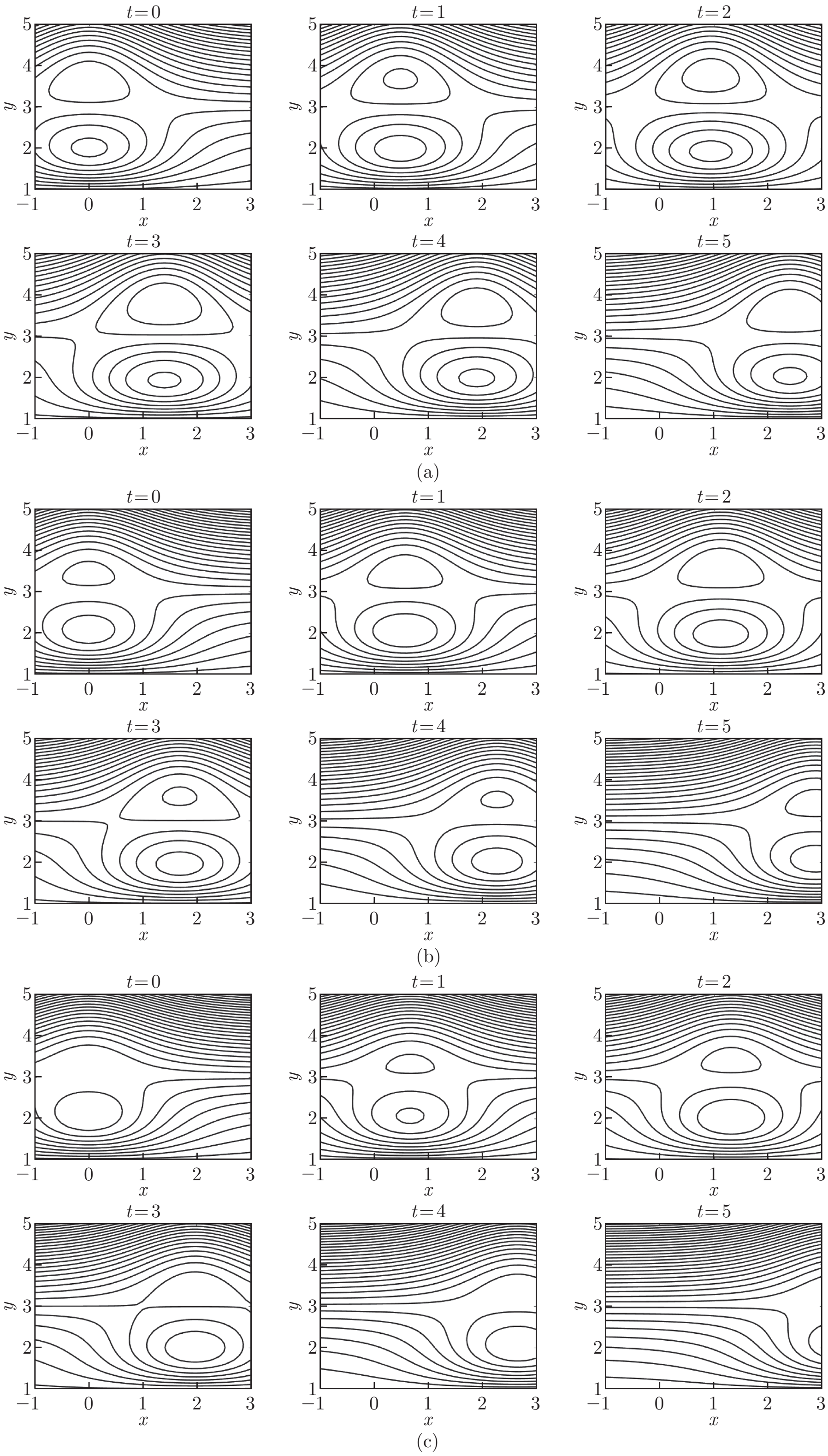

Fig. 2 Evolution of blocking under different background westerly flows: (a) $a_1 = -0.5$; (b) $a_1 = -0.6$; (c) $a_1 = -0.7$

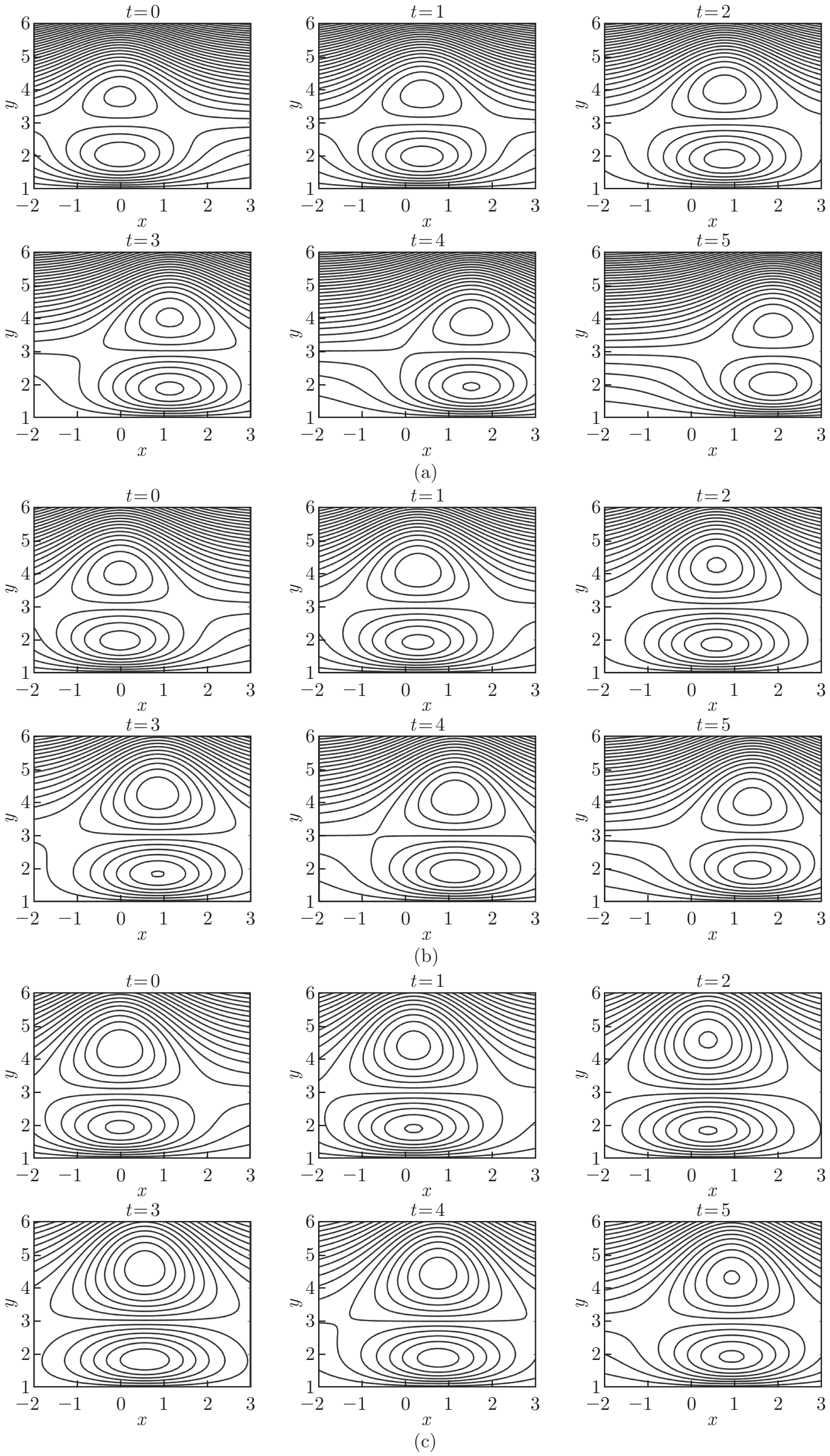

Fig. 3 Evolution of blocking under different background easterly flows: (a) $a_1 = -0.4$; (b) $a_1 = -0.3$; (c) $a_1 = -0.2$

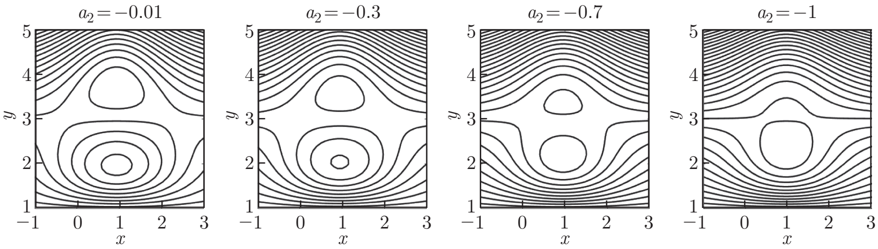

Fig. 4 Evolution of blocking under different westerly shears

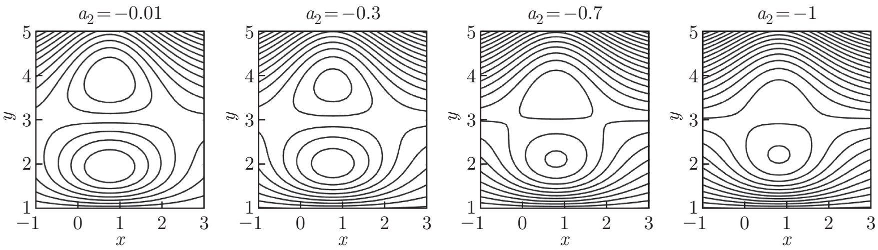

Fig. 5 Evolution of blocking under different easterly shears

3.3 Propagation of vortex

The vorticity expressed in the expression is the curl of velocity. It is a three-dimensional vector. The vertical component of vorticity is very important, and is called as vertical vorticity. What is analyzed in this part is the propagation of vertical vorticity, which is referred to as vorticity in the following analysis. Wu[45] discussed and gave the expression of (relative) vorticity in the z-coordinate system as follows:

$$\zeta = \frac{\partial v}{\partial x} - \frac{\partial u}{\partial y}. \tag{27}$$

He showed that vorticity is the rotational component of air particles relative to the ground around the zenith direction, owing to the uneven spatial distribution of horizontal motion. The vorticity of this paper can be obtained by substituting u and v we have mentioned earlier into Eq. (27),

$$\zeta = \nabla^2 \psi' - \frac{\partial \overline{u}}{\partial y} = \nabla^2 \psi_1 - \frac{\partial \overline{u}}{\partial y}. \tag{28}$$

Given the values of some parameters in Eq. (28), the same parameters can be used to obtain the evolution of vorticity over time. The results are shown in Fig. 8.

Two negative vorticity centers appear in Fig. 8, and the following conclusions can be obtained by comparison and analysis with Fig. 1. During the evolution from $t = 0$ to $t = 2$, Fig. 1 shows that the intensity of dipole blocking is increasing, and Fig. 8 shows that negative vorticity is increasing (the absolute value of negative vorticity is decreasing), which indicates that the rotational speed of air particles is decreasing. On the contrary, during the evolution from $t = 3$ to $t = 5$, Fig. 1 shows that dipole blocking is weakening, and Fig. 8 shows that negative vorticity is increasing (the absolute value of negative voticity is increasing), which indicates that the rotational speed of air particles is increasing. Thus, it can be assumed that the rotational speed of air particles is inversely proportional to the intensity of dipole blocking.

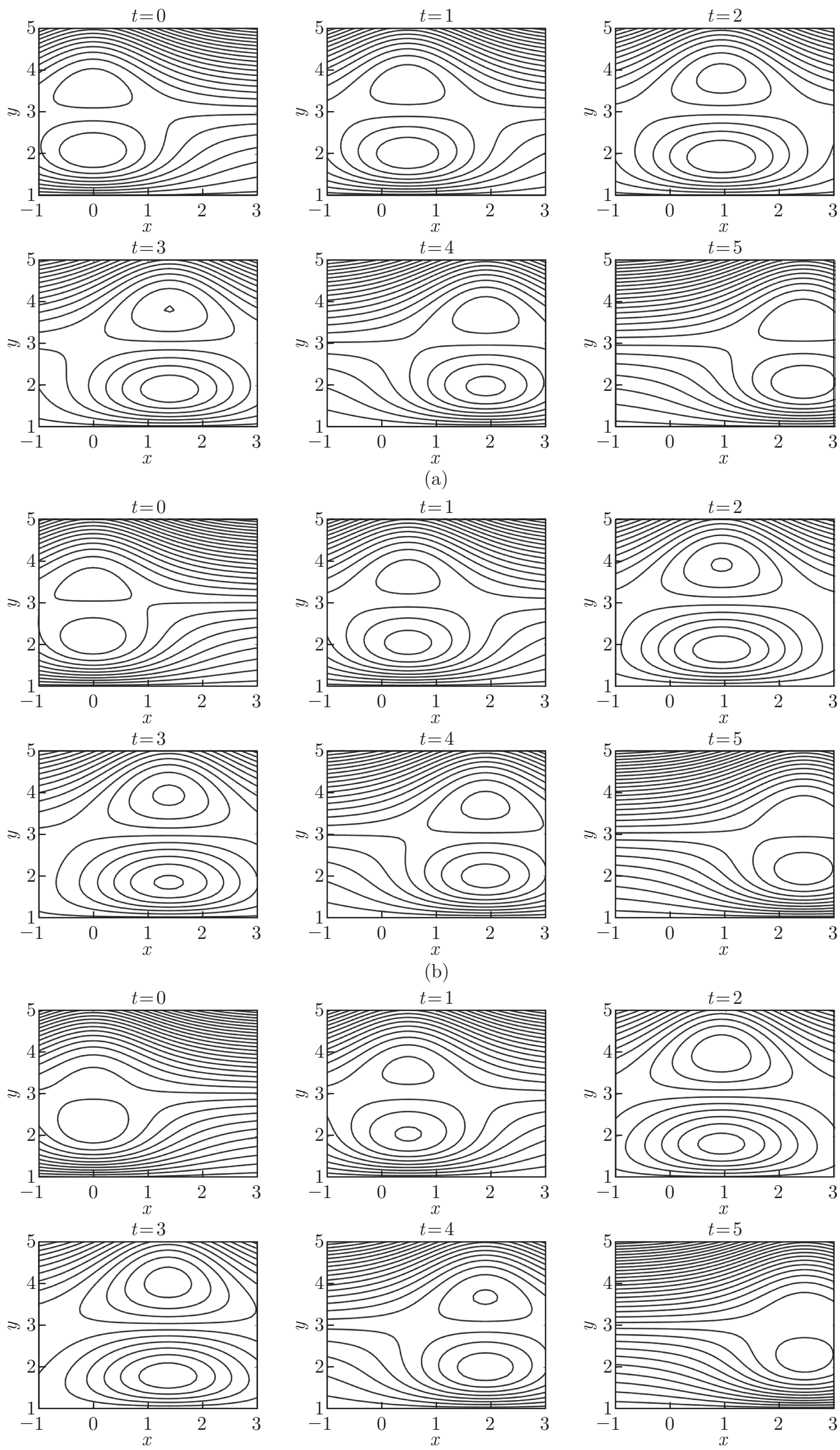

Fig. 6 Influence of time dependent westerly shear on dipole blocking: (a) $a_2 = -0.3\cos(1.2t)$; (b) $a_2 = -0.6\cos(1.2t)$; (c) $a_2 = -0.9\cos(1.2t)$

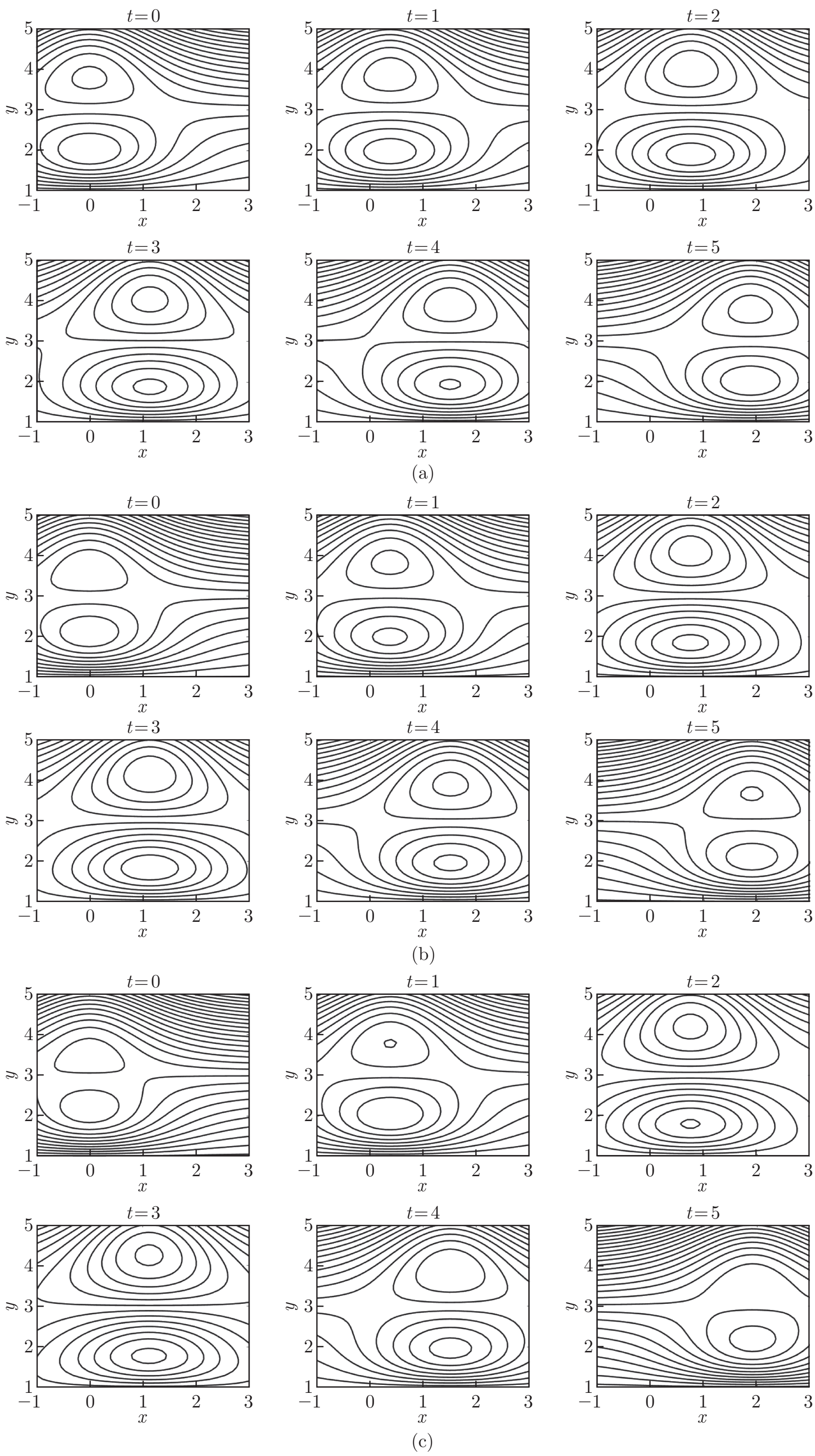

Fig. 7 Influence of time dependent easterly shear on dipole blocking: (a) $a_2 = -0.3\cos(1.2t)$; (b) $a_2 = -0.6\cos(1.2t)$; (c) $a_2 = -0.9\cos(1.2t)$

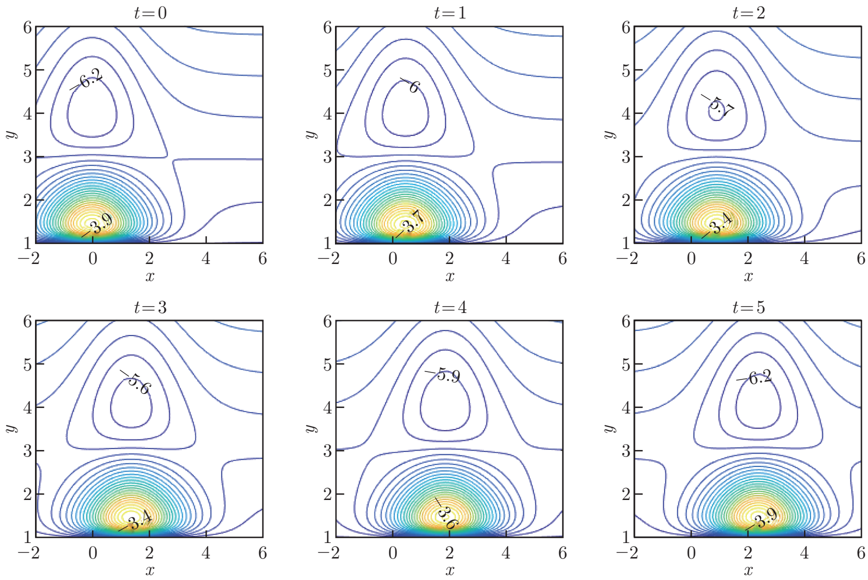

Fig. 8 Propagation of vortex under given parameters (color online)

4 Conclusions

In the last few decades, more and more investigations have been done on the understanding of physical mechanisms of atmospheric and oceanic motions. Large number of results highlight the essential importance of background flow in inducing the extreme weather events. In this paper, we have considered the effect of the time-dependent mean flow on the evolution of atmospheric blocking by the multi-scale technique. Through the above analysis, the following conclusions can be drawn.

(i) The background zonal flow is divided into the background easterly flow and the background westerly flow, and it can be concluded that their effects on dipole blocking are different. As the background westerly flow intensifies, the dipole blocking moves faster and decreases in intensity. However, when the background easterly flow intensifies, the movement speed of dipole blocking slows down and the intensity increases.

(ii) The shear of the background zonal flow is considered to be a constant or a time-dependent function. It can be seen that when the shear of background zonal flow is constant, the dipole blocking decreases with the increase in the shear. When the shear of background zonal flow is a time-dependent function, the formation, evolution, and decay of dipole blocking are more significant with the increase in the shear. Moreover, regardless of whether the shear is a constant or a time-dependent function, the intensity of dipole blocking under easterly shear is stronger than that under westerly shear.

(iii) With the increase in dipole blocking, the rotational speed of air particles decreases, and when the dipole blocking weakens, the opposite holds.

References

[1] PEDLOSKY, J. *Geophysical Fluid Dynamics*, 2nd ed., Springer-Verlag, New York (1987)

[2] ROSSBY, C. G. Relation between variations in the intensity of the zonal circulation of the atmosphere and the displacements of the semi-permanent centers of action. *Journal of Marine Research*, **2**(1), 38–55 (1939)

[3] CHARNEY, J. G. On the scale of atmospheric motions. *Geofysislw Publikasjoner*, **17**(2), 251–265 (1948)

[4] BERGGREN, R., BOLIN, B., and ROSSBY, C. G. An aerological study of zonal motion, its perturbations and break-down. *Tellus*, **1**(2), 14–37 (1949)

[5] LONG, R. R. Solitary waves in the westerlies. *Journal of the Atmospheric Sciences*, **21**(2), 197–200 (1949)

[6] REDEKOPP, L. G. and WEIDMAN, P. D. Solitary Rossby waves in zonal shear flows and their interactions. *Journal of the Atmospheric Sciences*, **35**(5), 790–804 (1978)

[7] CHARNEY, J. G. and DEVORE, J. G. Multiple flow equilibria in the atmosphere and blocking. *Journal of the Atmospheric Sciences*, **36**(7), 1205–1216 (1979)

[8] MCWILLIAMS, J. C. An application of equivalent modons to atmospheric blocking. *Dynamics of Atmospheres and Oceans*, **5**(1), 43–66 (1980)

[9] SHUTTS, G. J. The propagation of eddies in diffluent jetstreams: eddy vorticity forcing of 'blocking' flow fields. *Quarterly Journal of the Royal Meteorological Society*, **109**(462), 737–761 (1983)

[10] MALGUZZI, P. and MALANOTTE-RIZZOLI, P. Nonlinear stationary Rossby waves on nonuniform zonal winds and atmospheric blocking, part I: the analytica theory. *Journal of the Atmospheric Sciences*, **41**(17), 2620–2628 (1984)

[11] LUO, D. H. and JI, L. R. Observational study of dipole blocking in the atmosphere (in Chinese). *Chinese Journal of Atmospheric Sciences*, **15**(4), 52–57 (1991)

[12] LUO, D. H. Solitary Rossby waves in the rotating atmosphere and dipole blocking (in Chinese). *Acta Meteorologica Sinica*, **49**(4), 548–552 (1991)

[13] LUO, D. H. Planetary-scale baroclinic envelope Rossby solitons in a two-layer model and their interaction with synoptic-scale eddies. *Dynamics of Atmospheres and Oceans*, **32**(1), 27–74 (2000)

[14] LUO, D. H. Abarotropic envelope Rossby soliton model for block-eddy interaction, part I: effect of topography. *Journal of the Atmospheric Sciences*, **62**(1), 5–21 (2005)

[15] LUO, D. H., ZHANG, W. Q., ZHONG, L. H., and DAI, A. G. A nonlinear theory of atmospheric blocking: a potential vorticity gradient view. *Journal of the Atmospheric Sciences*, **76**(8), 2399–2427 (2019)

[16] LU, C. N., FU, C., and YANG, H. W. Time-fractional generalized Boussinesq equation for Rossby solitary waves with dissipation effect in stratified fluid and conservation laws as well as exact solutions. *Applied Mathematics and Computation*, **327**, 104–116 (2018)

[17] ZHANG, R. G. and YANG, L. G. Nonlinear Rossby waves in zonally varying flow under generalized beta approximation. *Dynamics of Atmospheres and Oceans*, **85**, 16–27 (2019)

[18] WANG, J., ZHANG, R. G., and YANG, L. G. Solitary waves of nonlinear barotropic-baroclinic coherent structures. *Physics of Fluids*, **32**(9), 096604 (2020)

[19] WANG, J., ZHANG, R. G., and YANG, L. G. A Gardner evolution equation for topographic Rossby waves and its mechanical analysis. *Applied Mathematics and Computation*, **385**, 125426 (2020)

[20] ZHANG, J. Q., ZHANG, R. G., YANG, L. G., LIU, Q. S., and CHEN, L. G. Coherent structures of nonlinear barotropic-baroclinic interaction in unequal depth two-layer model. *Applied Mathematics and Computation*, **408**, 126347 (2021)

[21] CIRO, D., RAPHALDINI, B., and RAUPP, C. F. M. Topography-induced locking of drifting Rossby-Haurwitz waves. *Physics of Fluids*, **32**, 046601 (2020)

[22] SHI, Y. L., YANG, D. Z., FENG, X. R., QI, J. F., YANG, H. W., and YIN, B. S. One possible mechanism for eddy distribution in zonal current with meridional shear. *Scientific Reports*, **8**(1), 10106 (2018)

[23] SHI, Y. L., YANG, D. Z., and YIN, B. S. The effect of background flow shear on the topographic Rossby wave. *Journal of Oceanography*, **76**, 307–315 (2020)

[24] SOLOMON, T. H., HOLLOWAY, W. J., and SWINNEY, H. L. Shear flow instabilities and Rossby waves in barotropic flow in a rotating annulus. *Physics of Fluids A: Fluid Dynamics*, **5**(8), 1971–1982 (1993)

[25] HODYSS, D. and NOLAN, D. S. The Rossby-inertia-buoyancy instability in baroclinic vortices. *Physics of Fluids*, **20**(9), 096602 (2008)

[26] KALASHNIK, M. V., CHKHETIANI, O. G., and KURGANSKY, M. V. Discrete SQG models with two boundaries and baroclinic instability of jet flows. *Physics of Fluids*, **33**, 076608 (2021)

[27] ZHANG, X. J., ZHANG, H. X., YANG, Y. Y., and SONG, J. Effect of quadric shear basic zonal flows and topography on baroclinic instability. *Tellus A*: *Dynamic Meteorology and Oceanography*, **72**(1), 1–9 (2020)

[28] YANG, Y. Y. and SONG, J. On the generalized eigenvalue problem of Rossby waves vertical velocity under the condition of zonal mean flow and topography. *Applied Mathematics Letters*, **121**, 107485 (2021)

[29] BERLOFF, P. S. and MCWILLIAMS, J. C. Quasigeostrophic dynamics of the western boundary current. *Journal of Physical Oceanography*, **29**(10), 2607–2634 (1998)

[30] POULIN, F. J. *The Instability of Time-dependent Jets*, Ph. D. dissertation, Massachusetts Institute of Technology, Massachusetts (2002)

[31] HUANG, F., TANG, X. Y., LOU, S. Y., and LU, C. H. Evolution of dipole-type blocking life cycles: analytical diagnoses and observations. *Journal of the Atmospheric Sciences*, **64**(1), 52–73 (2007)

[32] RADKO, T. Instabilities of a time-dependent shear flow. *Journal of Physical Oceanography*, **49**(9), 2377–2392 (2019)

[33] RADKO, T. Barotropic instability of a time-dependent parallel flow. *Journal of Fluid Mechanics* **922**, A11 (2021)

[34] YAN, X. M., KANG, D. J., CURCHITSER, E. N., and PANG, C. G. Energetics of dddy-mean flow interactions along the western boundary currents in the north pacific. *Journal of Physical Oceanography*, **49**, 789–810 (2019)

[35] NATAROV, A., RICHARDS, K. J., and MCCREARY, J. P. Two-dimensional instabilities of time-dependent zonal flows: linear shear. *Journal of Fluid Mechanics*, **599**, 29–50 (2008)

[36] PENG, K., ROTUNNO, R., and BRYAN, G. H. Evaluation of a time-dependent model for the intensification of tropical cyclones. *Journal of the Atmospheric Sciences*, **75**(6), 2125–2138 (2018)

[37] FAN, E. G. Connections among homogeneous balance method, Weiss-Tabor-Carnevale method and Clarkson-Kruskal method (in Chinese). *Acta Physica Sinica*, **49**(8), 1409–1412 (2000)

[38] SHEN, S. F. Clarkson-Kruskal direct dimilarity approach for differential-difference equations. *Communications in Theoretical Physics*, **44**(12), 964–966 (2005)

[39] LI, X. Z., ZHANG, J. L., and WANG, M. L. Solving KdV eauation with variable coefficients by using F-expansion method (in Chinese). *Journal of Yunnan University* (*Natural Sciences Edition*), **28**(3), 222–226 (2006)

[40] SHEN, S. J. Varied solitary wave solutions of KdV equation with variable coefficients (in Chinese). *Journal of Shaoxing University* (*Natural Sciences*), **32**(02), 12–16 (2012)

[41] LIU, S. S., FU, Z. T., LIU, S. D., and ZHAO, Q. Jacobi elliptic function expansion solution to the variable coefficient nonlinear equations (in Chinese). *Acta Physica Sinica*, **51**(9), 1923–1926 (2002)

[42] FU, Z. T., LIU, S. D., LIU, S. S., and ZHAO, Q. New exact solution to KdV equations with variable coefficients or forcing. *Applied Mathematics and Mechanics* (*English Edition*), **25**(1), 73–79 (2004) https://doi.org/10.1007/BF02437295

[43] LUO, D. H. Solitary Rossby waves with the Bata parameter and dipole blocking (in Chinese). *Quarterly Journal of Applied Meteorolog*, **6**(02), 220–227 (1995)

[44] LUO, D. H. and XU, H. The influence of background westerly wind on the formation of blocking by localized synoptic-scale eddies (in Chinese). *Journal of Ocean University of Qingdao* (*Natural Sciences Edition*), **32**(4), 501–510 (2002)

[45] WU, H. Comparison of the vorticity and divergence in two common meteorological coordinate systems (in Chinese). *Meteorological Monthly*, **47**(09), 1156–1161 (2021)